Supplementary Information

Band restructuring of ordered/disordered blue TiO_2 for visible photocatalyst

Simgeon Oh,‡[ac] Ji-Hee Kim,‡*[ac] Hee Min Hwang,[ac] Doyoung Kim,[ac] Joosung Kim,[ac] G. Hwan Park,[ab] Joon Soo Kim,[ac] Young Hee Lee*[ac] and Hyoyoung Lee*[ab]

[a]*Center for Integrated Nanostructure Physics (CINAP), Institute for Basic Science (IBS), Sungkyunkwan University, Suwon 16419, Korea*

[b]*Department of Chemistry, Sungkyunkwan University, Suwon 16419, Korea*

[c]*Department of Energy Science, Sungkyunkwan University, Suwon 16419, Korea*

‡These authors contribute equally to this work

*Corresponding authors

E-mail: kimj@skku.edu, leeyoung@skku.edu, hyoyoung@skku.edu

Fax: (+) 82-31-299-5934; Tel: (+) 82-31-299-4566

1. Phase-selective reduction in single-phase TiO_2

1.1 Crystalline structure

The phase-selectively reduced TiO_2 was carefully confirmed with single-phase TiO_2. The TiO_2 reductions were conducted using different alkali metal-ethylenediamine solutions. Single-phase anatase and rutile TiO_2 was reduced by lithium-ethylenediamine (Li-EDA) and sodium-ethylenediamine (Na-EDA) solutions, respectively (referred to as Li-reduction or Na-reduction). Each TiO_2 phase was reduced for 1, 3, 5 and 7 days to investigate the band structure as a function of reduction time.

XRD and TEM analyses were carried out to investigate the crystallographic modification resulting from Li and Na reduction. Fig. S1 shows the X-ray diffraction diffractometer (XRD) spectra of 6 samples: pristine anatase and rutile phase TiO_2, Li-reduced anatase and rutile phase TiO_2, and Na-reduced anatase and rutile phase TiO_2, each reduced for 7 days. These spectra showed the different reduction tendencies of anatase and rutile TiO_2 under our reduction reaction. In anatase TiO_2, the XRD peaks specific to anatase are unchanged with Li-reduction. However, these same peaks are barely evident when anatase is treated with Na-reduction. Meanwhile, rutile TiO_2 showed no XRD peak changes with Na-reduction, but the Li-reduced rutile sample showed decreased rutile peak intensities. Supplementary Table 1 shows the FWHM values of the (101) and (204) peaks in anatase TiO_2 and the (110) and (101) peaks in rutile TiO_2. High-resolution transmission electron microscopy (HRTEM) unveils ordered and disordered crystalline structures after Li- and Na-reduction, respectively (Fig. S2). These results imply that the TiO_2 disordering rates of Li- and Na-reduction are selectively effective for different TiO_2 crystalline phases. Thus, we denote Li-reduced TiO_2 as crystalline ordered anatase (A_o) and disordered rutile (R_d), and Na-reduced TiO_2 as crystalline disordered anatase (A_d) and ordered rutile (R_o).

1.2. Energy band structure

The energy band restructuring of Li- and Na-reduced single-phase TiO_2 samples were investigated by diffuse reflectance spectroscopy (DRS) and X-ray photoelectron spectroscopy (XPS) with different reduction times to observe the energy band change with respect to reduction level. DRS provides light absorption information and a deduced Tauc plot, which are essential for energy band gap measurements (Fig. S3). These data show that the anatase and rutile TiO_2 mainly absorb in the UV range due to their large energy band gaps of 3.2 eV and 3.0 eV, respectively, which is in good agreement with previous reports. After TiO_2 reduction treatment, the Li-reduced A_o and Na-reduced R_o show slightly increased absorption, but there is almost no bandgap change, while Na-reduced A_d and Li-reduced R_d show an enormous absorption increase in the visible spectrum. Furthermore, Na-reduced A_d and Li-reduced R_d show energy band tailing in the valence band, which was confirmed by XPS valence band analysis (Fig. S3). The measured energy band structures are summarized in Table S3, showing that our TiO_2 phase-selective reduction method successfully provides energy band restructuring.

2. Tables

Single-phase TiO_2	A(101)	A(204)	R(110)	R(101)
Pristine	0.3587°	0.5708°	0.1466°	0.1569°
7-day Li-reduction	0.4705°	0.8648°	0.4792°	0.5046°
7-day Na-reduction	1.4358°	2.0774°	0.1682°	0.1755°

Table S1. Full-width-at-half-maximum values of 7-day Li- and Na-reduced single-phase TiO_2. Anatase (101), (204) and rutile (110), (101) peaks are measured from single-phase TiO_2 XRD spectra (Fig. S1).

Phase-mixed TiO_2	A(101)	R(110)
Pristine	0.3755°	0.2576°
7-day Li-reduction	0.3726°	0.3921°
7-day Na-reduction	0.3942°	0.2450°

Table S2. Full-width-at-half-maximum variation of the XRD peaks of phase-selectively disordered anatase/rutile TiO_2 after Li- and Na-reduction.

	Li-reduction (Single-phase TiO_2)				Na-reduction (Single-phase TiO_2)			
Reduction time	Anatase (ordered, A_o)		Rutile (disordered, R_d)		Anatase (disordered, A_d)		Rutile (ordered, R_o)	
	VB (eV)	E_g (eV)	VB (eV)	E_g (eV)	VB (eV)	E_g (eV)	VB (eV)	E_g (eV)
0-day	2.11	3.18	2.00	3.01	2.11	3.18	2.00	3.01
1-day	2.09	3.2	2.00	2.98	2.09	3.15	2.02	3.00
3-day	2.09	3.19	1.85	2.96	1.94	3.09	1.96	3.00
5-day	2.11	3.17	1.78	2.93	1.85	2.91	2.01	2.98
7-day	2.05	3.16	1.72	2.88	1.87	2.73	2.00	2.98

Table S3. Measured valence band and energy band gap of single-phase TiO_2 with different Li- and Na-reduction times (Fig. S3).

	Phase reduction time				
	0-day (Pristine)	1-day	3-day	5-day	7-day
R_s (Li-reduction)	26.54 Ω	25.37 Ω	25.25 Ω	24.66 Ω	25.72 Ω
R_{ct} (Li-reduction)	55.16 kΩ	69.30 kΩ	73.49 kΩ	101.20 kΩ	158.10 kΩ
R_s (Na-reduction)	26.54 Ω	25.27 Ω	24.55 Ω	24.90 Ω	27.10 Ω
R_{ct} (Na-reduction)	55.16 kΩ	68.73 kΩ	140.50 kΩ	191.20 kΩ	181.17 kΩ

Table S4. Summarized R_s and R_{ct} values of Li-reduced (A_o/R_d) and Na-reduced (A_d/R_o) phase-mixed TiO_2 from the electrochemical impedance spectroscopy results (Fig. S14).

Photocatalyst	Structure	Photocatalysis parameters	H_2 generation rate	Reference
3-day Li-reduced P25	Nanoparticles	*No Pt loaded* 3:1 H_2O/MeOH (1 sun irradiation)	0.74 mmol g^{-1} h^{-1}	Our work
3-day Li-reduced Pt-P25	Nanoparticles	*0.04 wt.% Pt load* 3:1 H_2O/MeOH (1 sun irradiation)	6.84 mmol g^{-1} h^{-1}	Our work
Pt-P25	Nanoparticles	*0.46 wt.% Pt load* 4:1 H_2O/MeOH (1 sun irradiation)	5.71 mmol g^{-1} h^{-1}	Our work
Hydrogenated Pt-P25	Core/shell	*1.0 wt.% Pt load* 4:1 H_2O/MeOH (1 sun irradiation)	3.94 mmol g^{-1} h^{-1}	RSC Adv., 2014, 4, 1128–1132
Pt-anatase TiO_2	Core/shell	*0.5 wt.% Pt load* 4:1 H_2O/MeOH (1 sun irradiation)	7.40 mmol g^{-1} h^{-1}	Energy Environ. Sci., 2014, 7, 967–972
Pt-anatase TiO_2	Nanowires	*0.5 wt.% Pt load* 10:1 H_2O/MeOH (UV irradiation)	4.30 mmol g^{-1} h^{-1}	Catal Commun., 2008, 9, 1265-1271
Anatase-rutile Pt-composite	Nanoparticles	*0.4 wt.% Pt load* 10:1 H_2O/MeOH (300W Xe lamp)	4.25 mmol g^{-1} h^{-1}	J. Phys. Chem. C, 2010, 114, 2821–2829

Table S5. Summary of various Pt-loaded TiO_2 photocatalysts used for the photocatalytic hydrogen evolution reaction.

3. Figures

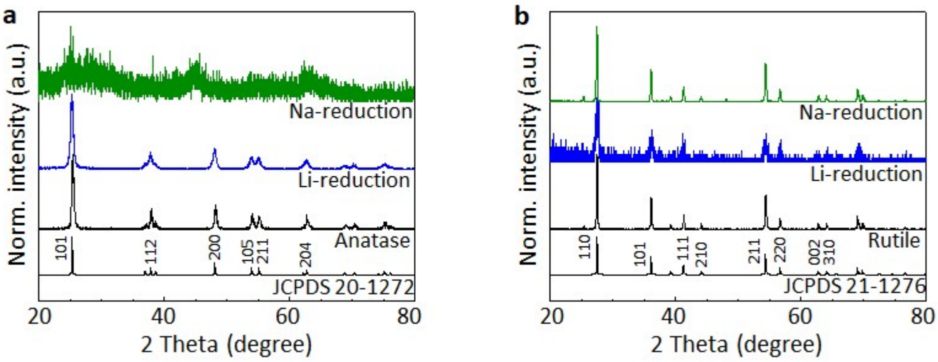

Fig. S1. XRD patterns of single-phase TiO_2 7-day Li- and Na-reduction, (a) anatase TiO_2 and (b) rutile TiO_2.

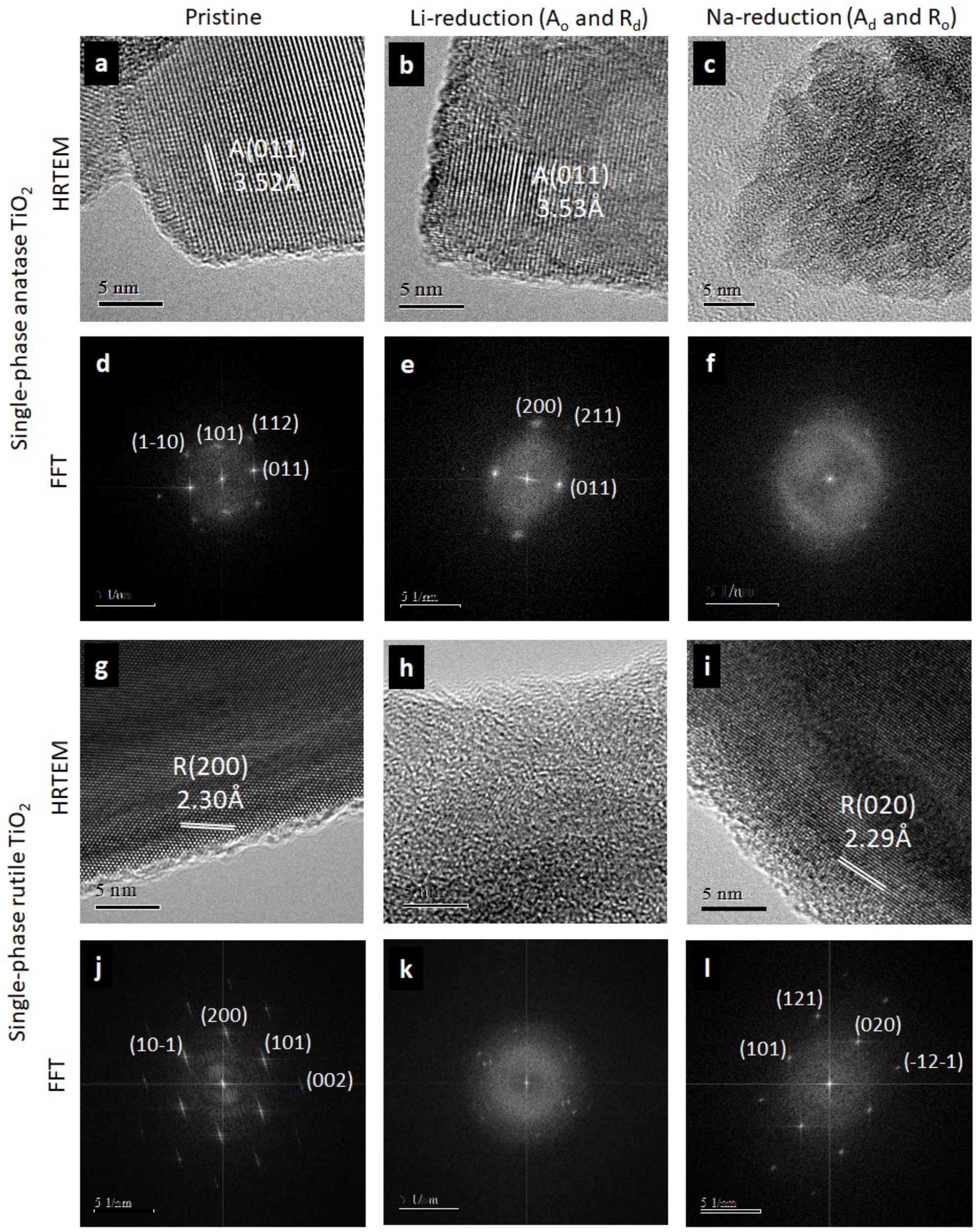

Fig. S2. HRTEM images of single-phase TiO_2. (a,d,g,j) without reduction, anatase phase (a) and rutile phase TiO_2 (g); corresponding electron-diffraction FFT pattern (d,j). (b,e,h,k) with the 7-day Li-reduction, anatase phase (b) and rutile phase TiO_2 (h); corresponding electron-diffraction FFT pattern (e,k). (c,f,i,l) with the 7-day Na-reduction, anatase phase (c) and rutile phase TiO_2 (i); corresponding electron-diffraction FFT pattern (f,l).

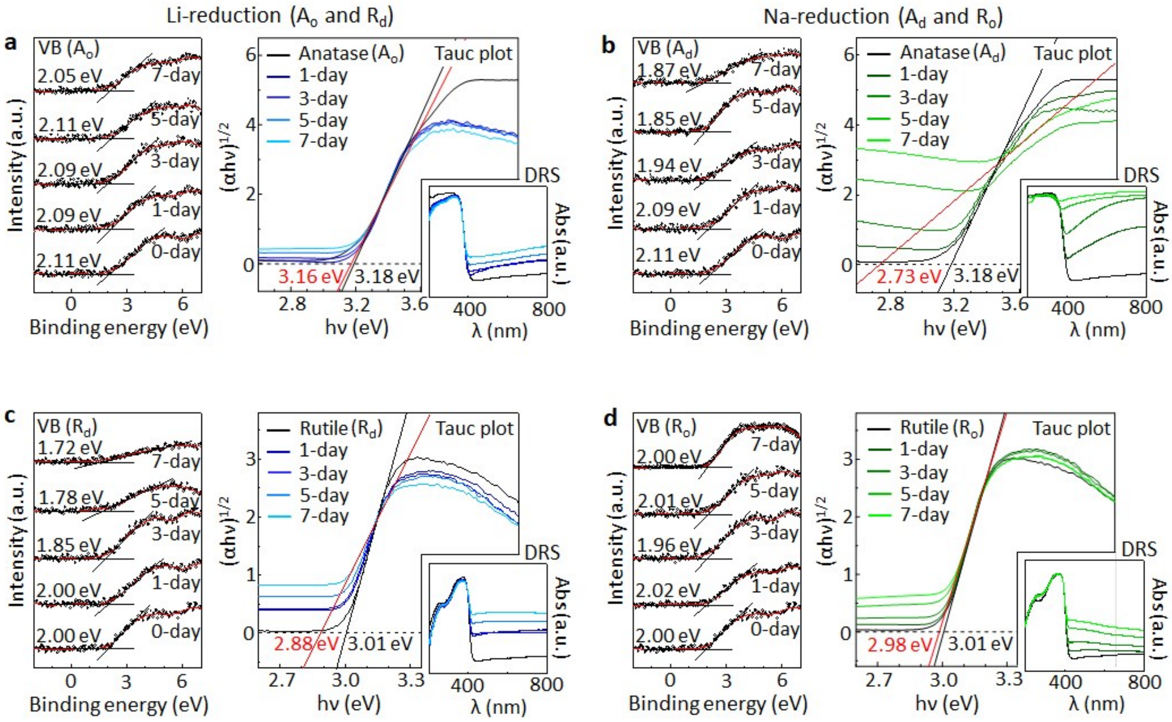

Fig. S3. Energy band structure survey with Li- and Na-reduced single-phase TiO_2. (a,c) XPS valence band (XPS VB) edge spectra and Tauc plot of single-phase TiO_2 with Li-reduction for anatase phase TiO_2 and rutile phase TiO_2 . (b,d) XPS VB edge spectra of single-phase TiO_2 with Na-reduction for anatase phase TiO_2 and rutile phase TiO_2. Inset: The DRS spectra.

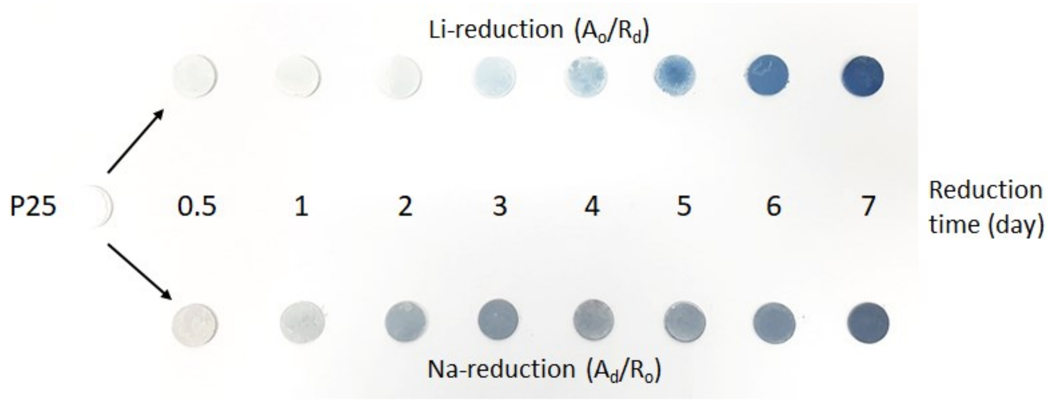

Fig. S4. Digital photograph images of pristine P25, Li-reduced (A_o/R_d, upper line) and Na-reduced (A_d/R_o, bottom line) phase-mixed TiO_2 with reduction time evolution. Both colors change from white to deep blue after reduction for 7 days.

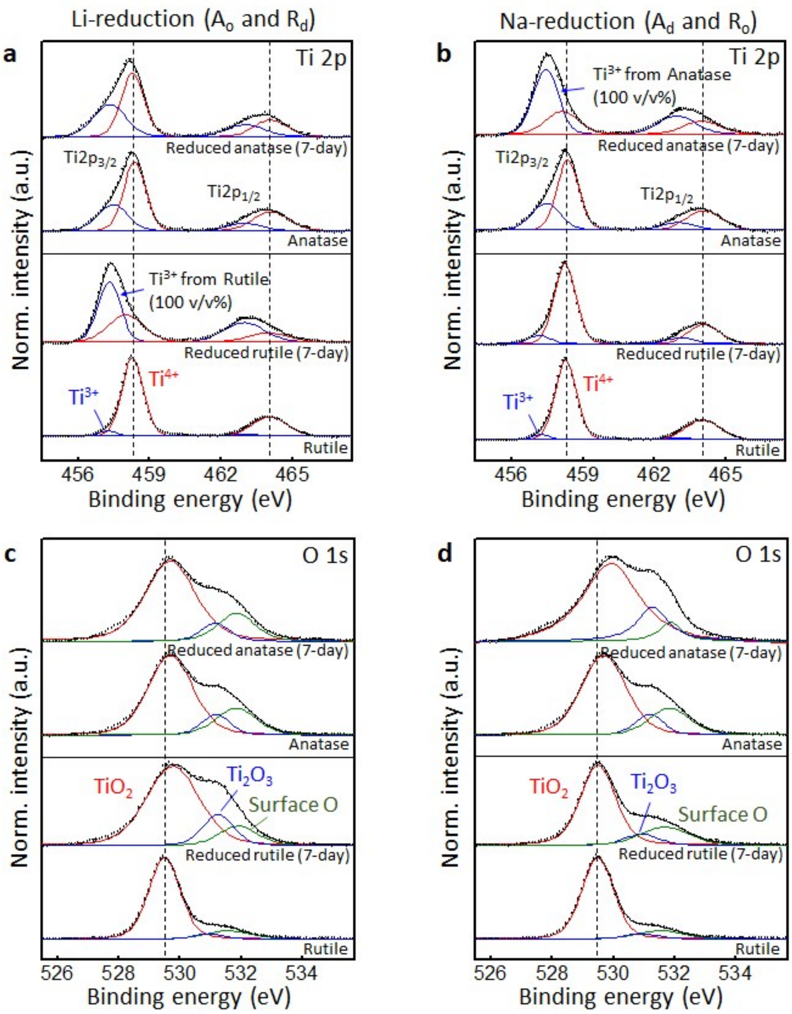

Fig. S5. (a,c) XPS core-level spectra of single-phase TiO_2 with 7-day Li-reduction: Ti 2p core-level XPS peaks and O 1s core-level XPS peaks. (b,d) XPS core-level spectra of single-phase TiO_2 with 7-day Na-reduction: Ti 2p core-level XPS peaks and O 1s core-level XPS peaks.

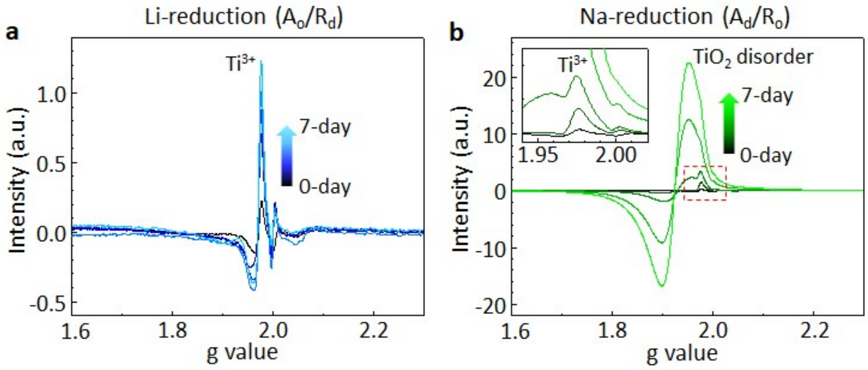

Fig. S6. EPR spectra of (a) Li-reduced and (b) Na-reduced anatase/rutile phase-mixed TiO_2 for the relative oxygen vacancies.

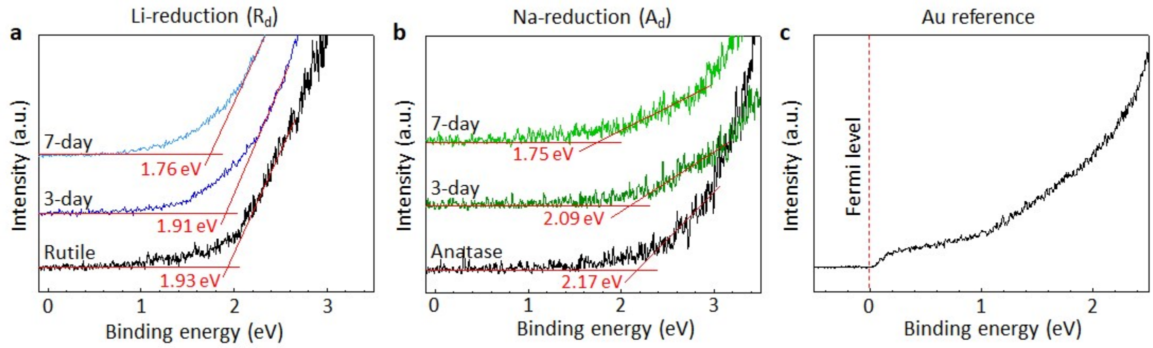

Fig. S7. UPS valence band spectra of (a) Li-reduced rutile TiO_2 (R_d) and (b) Na-reduced anatase TiO_2 (A_d) with reduction time evolution. (c) Fermi level reference with Au film.

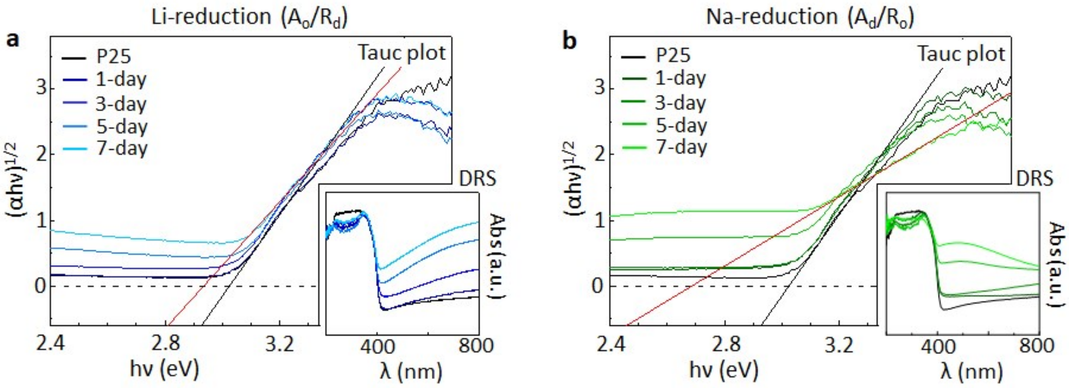

Fig. S8. (a) Tauc plots from UPS data, which are used to determine the direct bandgap via ~$(\alpha h\nu)^{1/2}$, of ordered anatase and disordered rutile phase-mixed TiO_2 with Li-reduction (A_o/R_d), and (b) disordered anatase and ordered rutile phase-mixed TiO_2 with Na-reduction (A_d/R_o). Inset: The DRS spectra.

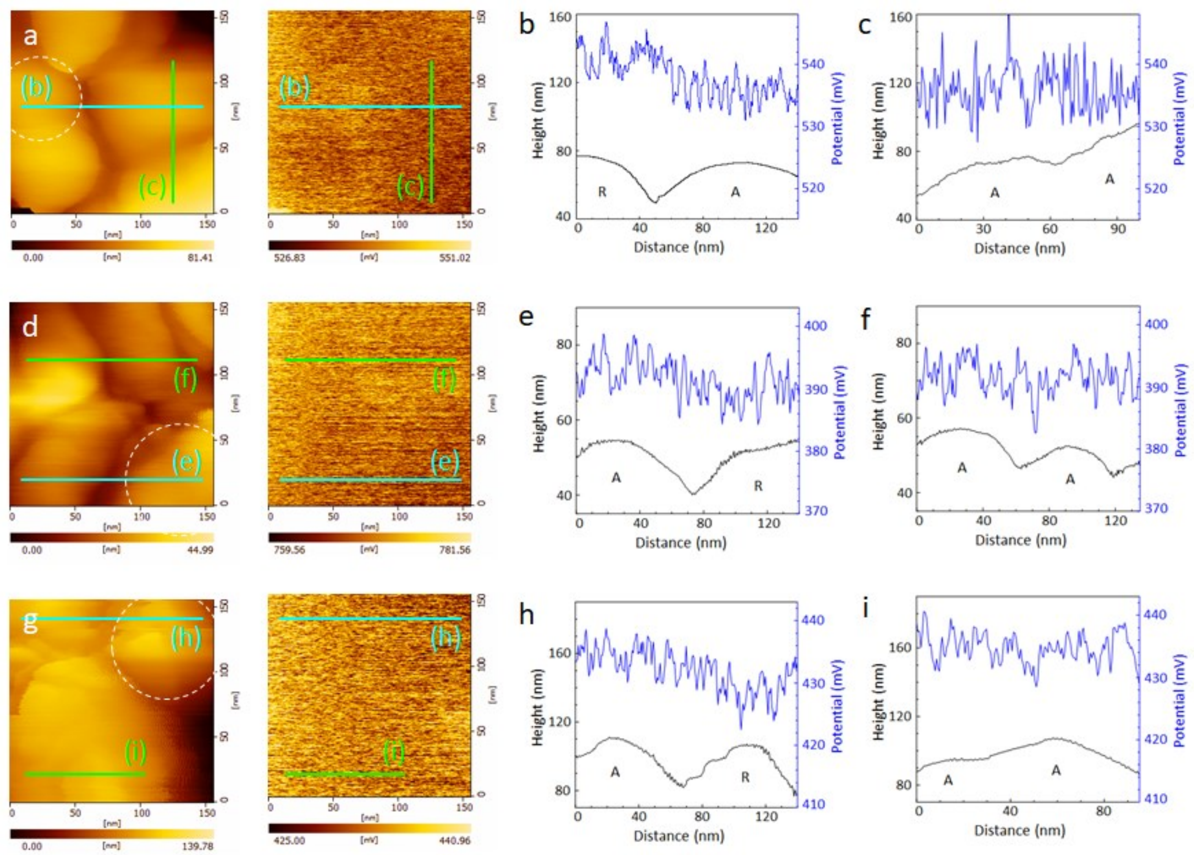

Fig. S9. AFM (left) and KPFM mapping (right) image of (a) pristine phase-mixed TiO_2, (d) 7-day Li- and (g) Na-reduced TiO_2. The line profile of (b, c) pristine phase-mixed TiO_2, (e, f) 7-day Li- and (h, i) Na-reduced TiO_2 for the anatase-rutile and anatase-anatase phase junction interfaces.

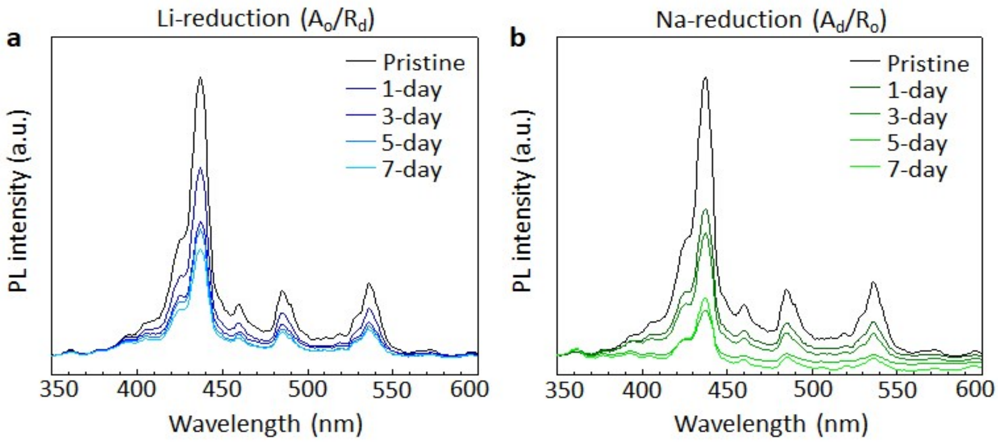

Fig. S10. PL spectra of (a) Li-reduced TiO_2 and (b) Na-reduced TiO_2 with different reduction time evolution.

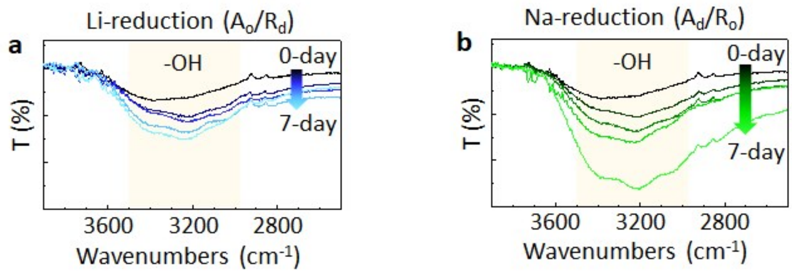

Fig. S11. FTIR spectra of phase-mixed TiO_2 with (a) Li-reduction (A_o/R_d) and (b) Na-reduction (A_d/R_o).

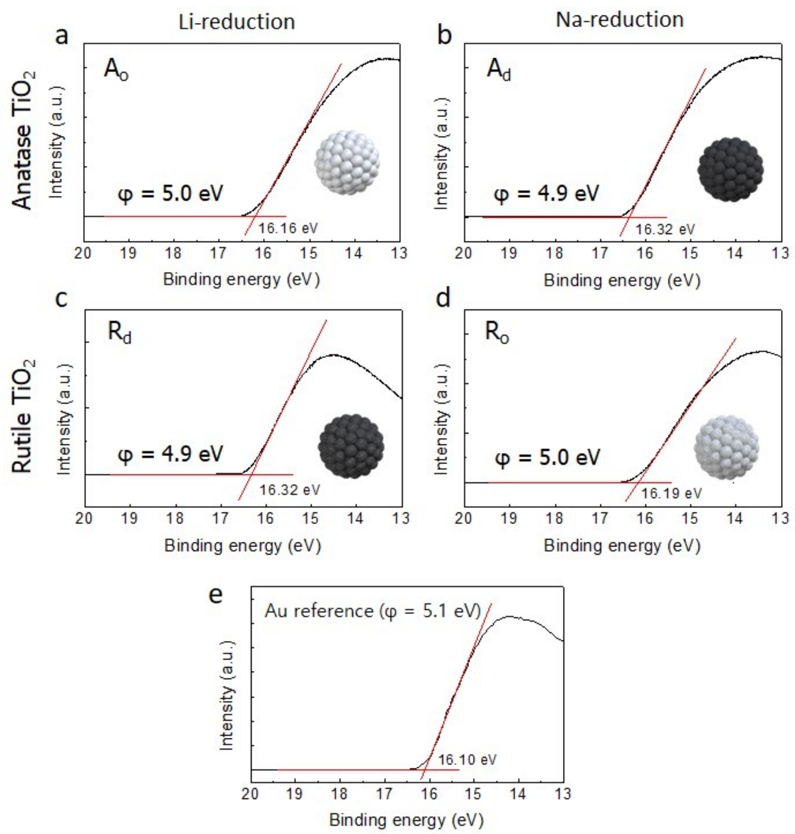

Fig. S12. The UPS cut-off region results for workfunctions measurement of single-phase TiO_2 after (a,c) 7-day Li-reduction and (b,d) 7-day Na-reduction. (e) UPS result of Au reference.

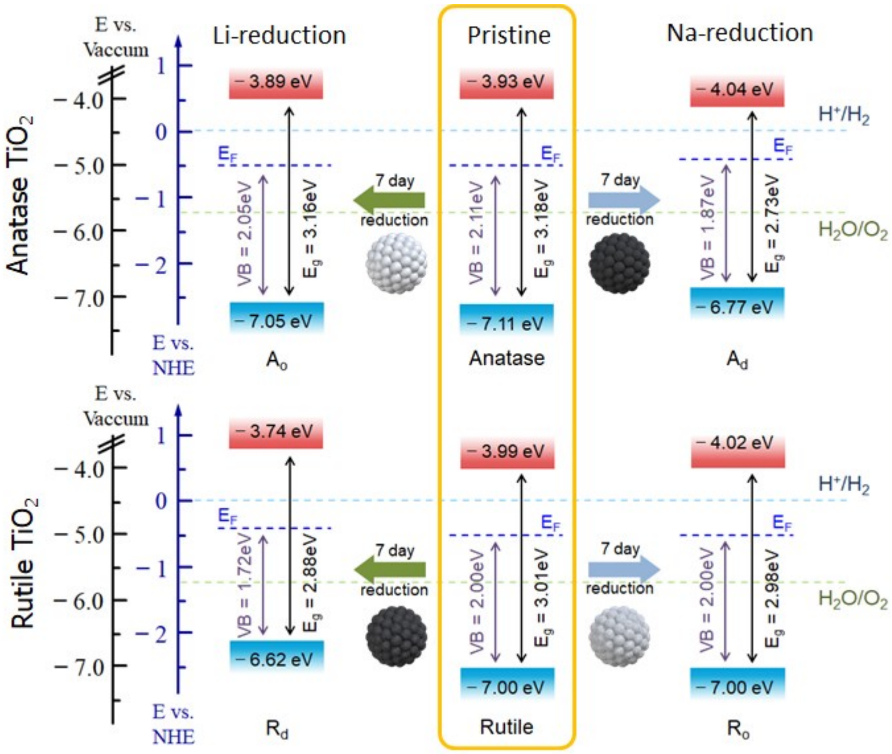

Fig. S13. Summarized energy band diagram of 7-day ordered and disordered single-phase TiO_2 to compare the CB position of TiO_2 and reduction potential of hydrogen for p-HER.

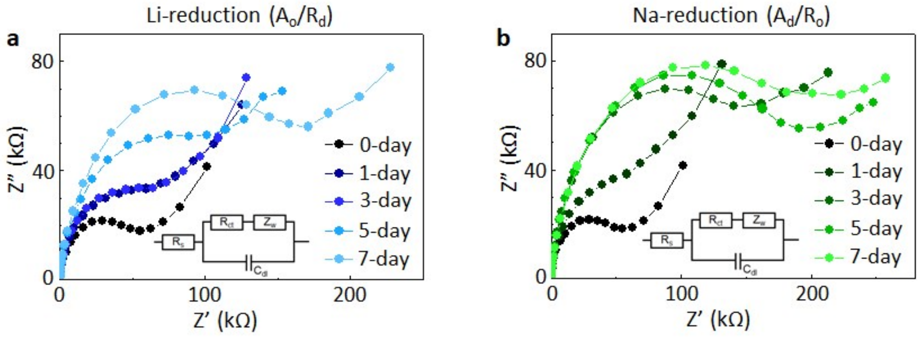

Fig. S14. Electrochemical impedance spectroscopy (EIS) spectra of phase-mixed TiO_2 with (a) Li-reduction (A_o/R_d), and (b) Na-reduction (A_d/R_o). Inset: The equivalent circuit model. R_s and R_{ct} values are served in Table S4.

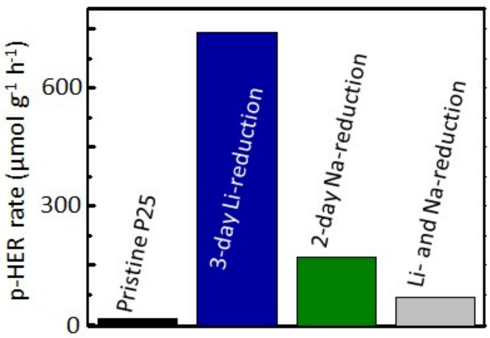

Fig. S15. p-HER results of pristine phase-mixed TiO_2 (P25) and phase-mixed TiO_2 with 3-day Li-reduction (A_o/R_d), 2-day Na-reduction (A_d/R_o), and 3-day Li- and then Na-reduction treatment (A_d/R_d).

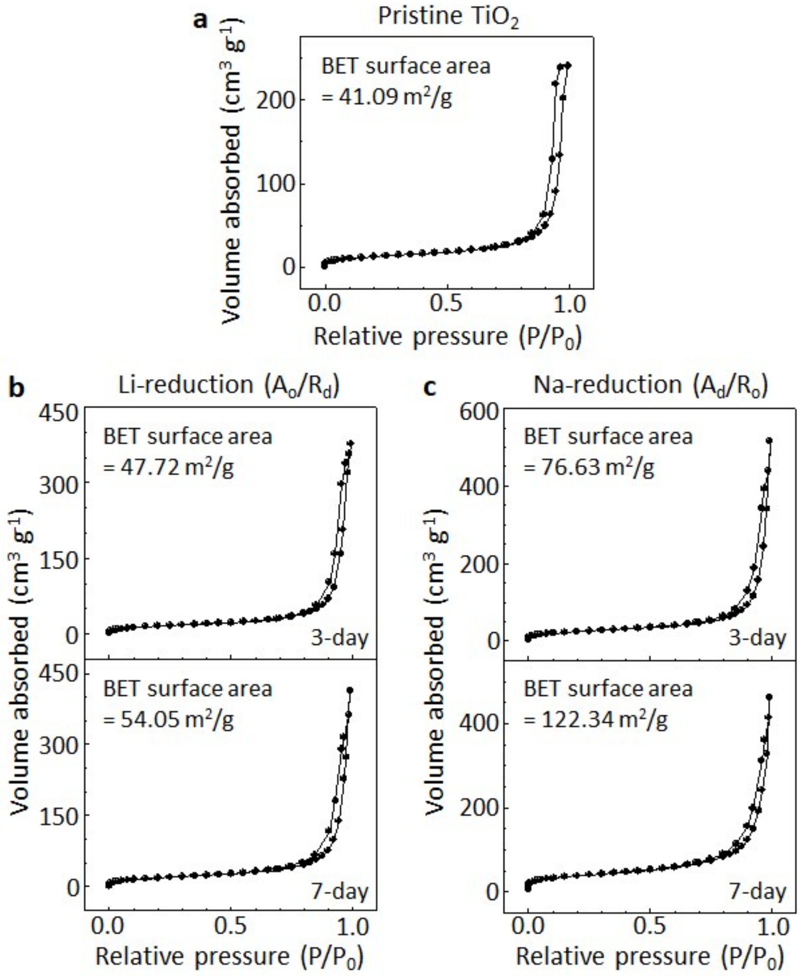

Fig. S16. N_2 adsorption–desorption isotherms of (a) Pristine P25 TiO_2, (b) Li-reduced TiO_2 and (c) Na-reduced TiO_2 as a function of the phase-selective TiO_2 reduction time.

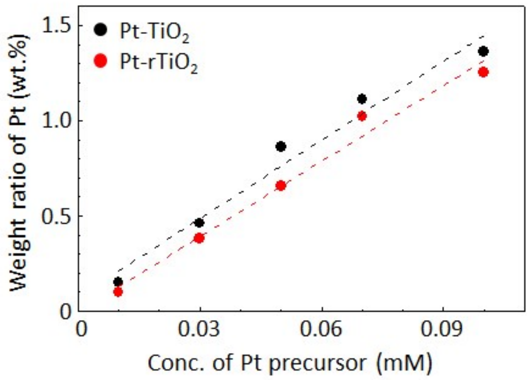

Fig. S17. Calibration curves of the weight ratio of Pt on Pt-TiO_2 and Pt-rTiO_2 with different concentrations of Pt precursor solution employed for photodeposition.

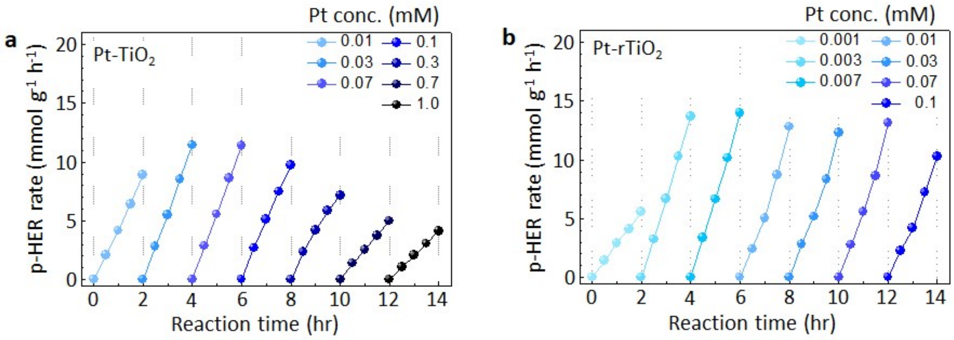

Fig. S18. p-HER performance as a function of Pt precursor concentration (mM) in the photodeposition solution with (a) Pt co-catalyst deposited on pristine P25 (Pt-TiO_2), and (b) phase-mixed TiO_2 with 3-day Li-reduction (Pt-rTiO_2).